Pergamon

Int. J. Solids Structures Vol. 32, No. 24, pp. 3573–3588, 1995

0020–7683/95 $9.50 + .00

0020–7683(95)00016–X

ANALYSIS OF THE TENSILE STRENGTH OF PARALLEL-LAY ROPES AND BUNDLES OF PARALLEL ELEMENTS BY PROBABILITY THEORY

G. AMANIAMPONG

Solid Mechanics Division, Faculty of Engineering, University of Waterloo, Waterloo, Ontario, Canada N2L 3G1

and

C. J. BURGOYNE

Engineering Department, University of Cambridge, Trumpington Street, Cambridge CB2 1PZ, U.K.

(*Received* 20 *January* 1993; *in revised form* 5 *January* 1995)

Abstract—A model for determining the tensile strength of parallel-lay ropes and bundles of parallel elements by means of a probability theory is presented. Ropes of a characteristic length are modelled from the knowledge of the statistical properties of the constituent elements and the weakest-link concept is employed to extend the results to long ropes. From the model, analysis of parallel-lay ropes with non-linear stress–strain relationships can be carried out and the study of the variability effects on the ropes, due to the scatter in elements' characteristics, is permitted. The variability in the element stiffness has a profound effect on the bundle strength. The scatter in the element cross-sectional area increases the bundle strength slightly, albeit by an insignificant amount. The results from the model are contrasted with classical bundle theory, and experimental data from parallel-lay ropes made from Kevlar-49 aramid and high tenacity polyester yarns have been used to predict, with reasonable accuracy, the tensile strength behaviour of the ropes.

1. INTRODUCTION

Over the last few decades, progress in the polymer industry has led to the production of materials with many desirable mechanical properties. These materials have found applications in diverse areas such as the civil and aeronautical engineering industries.

In the civil engineering industry, parallel-lay ropes made from high strength synthetic fibres may soon be preferred for use in many offshore and bridge structures. They have many advantages over steel and other traditional materials used in construction and could be used to replace high tensile steel tendons and strands in many application areas, particularly where low weight and corrosion resistance are of prime concern (Burgoyne, 1988). Parallel-lay ropes have also been identified for use in cable stayed and suspension bridges, cable supported roofs, prestressed concrete structures, deep water platforms, prestressed brickwork and retaining walls (Burgoyne, 1988; Kingston, 1988; Lane and Kempton, 1988; Baxter, 1988).

Of all the various types of rope construction, parallel-lay ropes give the best conversion efficiency from the properties of the elements to those of the ropes (Kingston, 1988). They are composed of yarns which are laid parallel to each other and to the axis of the rope throughout the entire rope length; unlike twisted-lay (stranded) or braided rope construction, where serpentine or helical yarn paths are introduced, maximum use of the yarn strength is achieved and the full stiffness of the constituent yarns is mobilized. Because of the parallel construction, adverse properties such as low tension–tension fatigue performance and abrasion, which are associated with the other forms of rope construction, are avoided.

Parafil ropes are a type of parallel-lay rope made by Linear Composites Ltd. They consist of parallel filaments contained within a non-structural polymeric sheath. A number

of different yarns can be used in the core, but those ropes containing Kevlar-49, known as Type G, or polyester, known as Type A, are of relevance here. All the tests referred to in this work [and also that of Chambers (1986) and Guimarães (1988b)] were carried out on these ropes, or yarns taken from such ropes.

In parallel construction, the ability of broken elements to shed load to their neighbours is greatly reduced; this is achieved in structured ropes by friction between adjacent elements. There is little interaction between the individual yarns, and the ropes can be seen as an aggregate of separate elements. However, the tensile strengths of the ropes are not accurately predicted from the elements by simple averaging rules. This effect is more pronounced when the elements are elastic, with high stiffness, as is typical in high performance ropes, and also increases with variability in element strength. A random sample of apparently identical elements shows a large scatter in strength and this has a profound effect on the strength of the resulting bundle or rope (Pitt and Phoenix, 1981). The tensile strength efficiency (the ratio of the bundle strength to the mean strength of elements) of fibre bundles decreases monotonically with the increase in the element coefficient of variation (ratio of element standard deviation to the mean strength) (Coleman, 1958). The variability in strength of materials is attributed to flaws which are randomly distributed within the bulk of the materials (Griffith, 1921). Thus, the failure event can be modelled as a stochastic process and the probabilistic approach is adopted here.

Daniels (1945) used a stochastic process and studied bundles of thread made by parallel construction; this is now generally referred to as the classical bundle theory. Daniels developed an asymptotic result for such a rope, but the model was simple in that it only applied to ropes with linear elastic elements and the only variable parameter was the strength of the constituent elements. An application of Daniels' classical model to Parafil Type G ropes by Chambers (1986) was unable to explain the rope behaviour.

Phoenix and Taylor (1973) and Phoenix (1974, 1975) considered more realistic models of bundles of parallel elements where the strain of the elements, rather than the stress, was used as the main statistical parameter. They introduced random slack into the model but kept other parameters constant and developed an asymptotic result. This gives a specific value for the bundle strength, but it has been observed by Guimarães (1988a, b) that there is a size effect associated with Type G ropes.

In the models described above, fibres with linear stress–strain relationships and with the same cross-sectional area, stiffness and stress–strain curve are assumed; however, tensile tests of polymeric fibres show that fibres exhibit a large scatter in their cross-sectional areas, and their stiffnesses do vary (Wagner *et al.*, 1984; Chambers, 1986; Wagner, 1989). A fibre continuum study of bundles with linear elastic elements with linearly varying stiffnesses also shows that the variation in the element stiffness may have a profound effect on the strength of bundles of parallel elements (Hult and Travnicek, 1983). The variability in the stiffness of the bundle elements can therefore not be ignored.

In this paper, a probabilistic model which can be used to predict the tensile strength of bundles of parallel elements and parallel-lay ropes from the knowledge of the properties of the constituent elements is presented. The cross-sectional area, the breaking strain and the stiffness of the bundle elements, as well as the slack, are assumed as random variables. The scatter in the elements' characteristics is then taken into account in order to study the variability effect. The restriction on the element stress–strain behaviour is also relaxed so that a polynomial can be used to represent the stress–strain behaviour, which allows the model to be applied to ropes with non-linear stress–strain behaviour. To extend the model to large ropes, the recently developed asymptotic result by Daniels (1989) is employed and the convergence is compared with Monte-Carlo simulations.

The assumptions governing the probabilistic model do not remain valid when long ropes are considered. As the length of the rope increases so does the interaction between the elements, and the rope can no longer be considered as a bundle of parallel independent elements. A long rope is therefore modelled in this paper as a series of small sub-bundles with parallel elements. The length of the sub-bundles is considered as the characteristic length of the rope. The weakest link concept is then employed to predict the strength of long ropes.

The authors are indebted to one of the reviewers of the paper for drawing to their attention a work published after the original manuscript was prepared. Harlow and Yukich (1993) used function-indexed empirical processes and deduced central limit theorems applicable to fibre bundles. Their approach allows for a variety of new applications and generalizations which are not obtained from previous studies.

2. BUNDLE STRENGTH

2.1. *Assumptions and formulation of the model*

Consider a bundle of n parallel elements (members) of the same type with varying cross-sectional areas and stiffnesses. Assume that the bundle is clamped in such a way that the elements have different slacks, and that load is applied to the bundle by means of extension. Let the force–strain relationship of each element be governed by an mth order polynomial. Thus, the force–strain relationship of an element is given by

$$\varphi(a, \underline{\alpha}^t, \lambda) = a \sum_{k=1}^{m} \alpha_k \lambda^k, \tag{1}$$

where a is the element cross-sectional area and the vector $\underline{\alpha}^t = (\alpha_1, \ldots, \alpha_m)$ represents the coefficients of the polynomial of stress against strain.

If $Z_i(\varepsilon)$ is the force in the ith element at bundle strain, ε, and θ_i the initial slack strain of the element, then

$$Z_i(\varepsilon) = \begin{cases} 0 & 0 \leqslant \varepsilon < \theta_i \\ a_i \Sigma_{k=1}^{m} \alpha_{ik} (\varepsilon - \theta_i)^k & \theta_i \leqslant \varepsilon < \theta_i + \zeta_i \\ 0 & \varepsilon \geqslant \theta_i + \zeta_i, \end{cases} \tag{2}$$

where ζ_i is the failure strain of the element i and a_i is the cross-sectional area of element i.

Assume that the element failure strains, $\zeta_1, \ldots, \zeta_n$, slack strains, $\theta_1, \ldots, \theta_n$, cross-sectional areas, $a_1, \ldots, a_n$, and the coefficients of the polynomials $\underline{\alpha}_1^t, \ldots, \underline{\alpha}_n^t$ are each independent identically-distributed random variables with the density functions (dfs) and cumulative distribution functions (cdfs) shown in Table 1.

Assume also that for each element i, $\{\zeta_i, \theta_i, a_i, \underline{\alpha}_i^t\}$ are jointly distributed but independent for the successive sets $\{\zeta_1, \theta_1, a_1, \underline{\alpha}_1^t\}, \{\zeta_2, \theta_2, a_2, \underline{\alpha}_2^t\} \ldots$.

The bundle load at bundle strain ε is given by

$$L_n(\varepsilon) = \sum_{i=1}^{n} Z_i(\varepsilon) \tag{3}$$

and the bundle strength is $S_n^* = L_n^*/n\mu_a$, where L_n^* is the maximum value achieved by $L_n(\varepsilon)$, i.e. sup $\{L_n(\varepsilon); \varepsilon \geqslant 0\}$ and μ_a is the mean element area. If $F(\zeta, \theta, a, \underline{\alpha}^t)$ is the joint distribution function of the parameters $\zeta_i, \theta_i, a_i, \underline{\alpha}_i^t$, then the mean element load at bundle strain, ε, is given by

Table 1. Distribution functions for parameters of the analysis

Random variable	df	cdf
ζ	$h(\zeta)$	$H(\zeta)$
θ	$g(\theta)$	$G(\theta)$
a	$j(a)$	$J(a)$
$\underline{\alpha}^t$	$b(\underline{\alpha}^t)$	$B(\underline{\alpha}^t)$

$$\mu(\varepsilon) = E[Z_i(\varepsilon)] = \int \varphi[a, \underline{\alpha}^t, (\varepsilon - \theta)]\, \mathrm{d}F(\zeta, \theta, a, \underline{\alpha}^t), \tag{4}$$

where $E[x]$ is the expected value of the variable x, and the covariance function is expressed as

$$\Psi(\varepsilon_1, \varepsilon_2) = \mathrm{Cov}\,[Z_i(\varepsilon_1), Z_i(\varepsilon_2)], \quad \varepsilon_1 \geqslant 0, \quad \varepsilon_2 \geqslant 0. \tag{5}$$

From the definition of covariance we get

$$\Psi(\varepsilon_1, \varepsilon_2) = E[Z_i(\varepsilon_1) Z_i(\varepsilon_2)] - \mu(\varepsilon_1)\mu(\varepsilon_2). \tag{6}$$

Equation (6) can also be written as

$$\Psi(\varepsilon_1, \varepsilon_2) = \int \varphi[a, \underline{\alpha}^t, (\varepsilon_1 - \theta)]\varphi[a, \underline{\alpha}^t, (\varepsilon_2 - \theta)]\, \mathrm{d}F(\zeta, \theta, a, \underline{\alpha}^t) - \mu(\varepsilon_1)\mu(\varepsilon_2). \tag{7}$$

In order to simplify the analysis the following assumptions are also made:

(1) the distributions of the random variables ζ, θ, a and α^t are independent;
(2) the coefficients of the polynomial $\underline{\alpha}^t$ of each element are dependent and are related by a multinormal distribution.

The first assumption is made for simplification purposes. It is also unlikely that a joint distribution function for all the parameters involved could be obtained. Neither is it likely to expect any reliable data on dependencies. The second assumption is made because it is unsatisfactory to consider the coefficients of the polynomial of each element as independent. Although there is no physical justification for choosing a multinormal distribution, it is the most widely used multivariate distribution.

It is then possible to replace $F(\zeta, \theta, a, \underline{\alpha}^t)$ by the product of the different cumulative distribution functions (H, G, J and B) and eqns (4) and (7) can then be written (Amaniampong, 1992) as:

$$\mu(\varepsilon) = \mu_a \int_0^{\min(\varepsilon, \theta_{\max})} \left\{ \int \cdots \int \sum_{i=1}^{m} \alpha_i (\varepsilon - \theta)^i \, \mathrm{d}B(\underline{\alpha}^t) \right\} [1 - H(\varepsilon - \theta)]\, \mathrm{d}G(\theta) \tag{8}$$

and

$$\Psi(\varepsilon_1, \varepsilon_2) = \mu_{2a} \int_0^{\min(\varepsilon_1, \theta_{\max})} \left\{ \int \cdots \int \left[\sum_{i=1}^{m} \alpha_i (\varepsilon_1 - \theta)^i \right] \times \left[\sum_{i=1}^{m} \alpha_i (\varepsilon_2 - \theta)^i \right] \mathrm{d}B(\underline{\alpha}^t) \right\} [1 - H(\varepsilon_2 - \theta)]\, \mathrm{d}G(\theta) - \mu(\varepsilon_1)\mu(\varepsilon_2), \tag{9}$$

where $\theta_{\max}$ is the maximum value of the slack strain, $\varepsilon_1 \leqslant \varepsilon_2$ and $\mu_{2a} = \int a^2\, \mathrm{d}J(a)$.

The bundle strength can then be evaluated by one of the following methods.

(1) Exact solution: properties are assigned to each element and recursive formulae are derived to solve the problem. Unfortunately, the mathematical complexities and the accumulation of rounding errors in the subsequent calculations required even to evaluate the strength of bundles with a small number of elements, and even in the "simple" case of the classical bundle, make the method impractical (Daniels, 1945; Phoenix, 1974), and it is not used here.

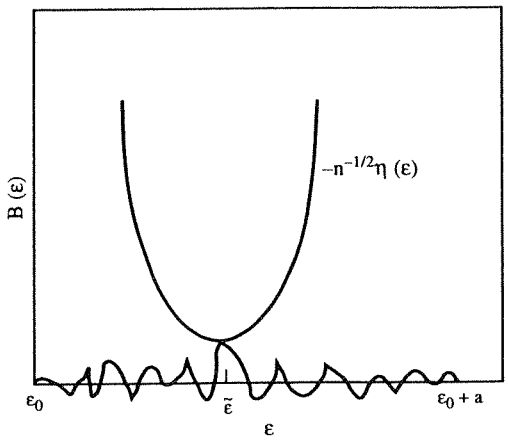

Fig. 1. Brownian bridge $B(\varepsilon)$ on $(\varepsilon, \varepsilon_0+a)$ superimposed on the curve $-n^{1/2}\eta(\varepsilon)$.

(2) Asymptotic method : this method applies to bundles of a large number of elements. The failure process is superimposed on a curve near its maximum to evaluate the bundle strength.

(3) Monte-Carlo simulation : the outcome of a process can be observed by randomly assigning a value to an underlying variable. Such a practice is referred to as a Monte-Carlo experiment. A Monte-Carlo simulation is then composed of, say, n such independent experiments and by the virtue of the law of large numbers, observations made from a sufficiently large number of the experiments will give a good measurement of the statistical characteristics of the process. The failure process is therefore simulated by randomly assigning properties to the elements to evaluate the bundle strength. The procedure is repeated many times and statistical inferences are made about the bundle strength.

2.2. *Asymptotic method*

Since the bundle strength is dictated by the maximum value achieved by $L_n(\varepsilon)$, one would expect the strength to be given by $S_n^* = \sup\{\mu(\varepsilon)/\mu_a, \varepsilon \geqslant 0\}$. However, this is not the case, and for bundles of large number of elements, the results obtained by Daniels (1989) on a Gaussian process whose mean path has a maximum are employed. The asymptotic distribution of the bundle failure load and extension are deduced from the results for the maximum, and the time at which the maximum is attained, of a general Gaussian process superimposed on a parabolic curve near its maximum (Daniels, 1989).

The covariance function, eqn (9), can be converted to a statistical process given by

$$\Psi(\varepsilon_1, \varepsilon_2) = C(\varepsilon_1 - \varepsilon_0)[1 - (\varepsilon_2 - \varepsilon_0)/\delta], \tag{10}$$

where $C > 0$ and $\varepsilon_0 \leqslant \varepsilon_1 \leqslant \varepsilon_2$. The following cases are then identified :

(1) when $\delta = \infty$ the process is a Brownian motion on (ε_0, ∞) ;
(2) when $\delta > 0$ the process is a Brownian bridge on $(\varepsilon_0, \varepsilon_0+\delta)$; and
(3) when $\delta < 0$ the process is proportional to a process Y analogous to a Brownian bridge.

A Brownian motion $W(t)$ on $(0, \infty)$ is a stochastic process with $W(0) = 0$, mean $E[W(t)] = 0$ and covariance function $\mathrm{Cov}[W(t_1), W(t_2)] = t_1$ for $t_1 \leqslant t_2$. A Brownian bridge $B(t)$ on $(0, T)$ is also a stochastic process with mean $E[B(t)] = 0$ and covariance function $\mathrm{Cov}[B(t_1), B(t_2)] = t_1(1-t_2/T)$, $t_1 \leqslant t_2$, whereas the process $Y(t)$ analogous to a Brownian bridge on $(0, T)$ is such that the mean is given as $E[Y(t)] = 0$ and the covariance function $\mathrm{Cov}[Y(t_1), Y(t_2)] = t_1(1+t_2/T)$, $t_1 \leqslant t_2$. Details of these processes can be found in Karlin and Taylor (1981).

By superimposing the process in eqn (10) on a curve $-n^{1/2}\eta(\varepsilon)$ which has its minimum at $\tilde{\varepsilon}$ (Fig. 1), where $\eta(\tilde{\varepsilon}) = 0$ and the first derivative $\eta'(\tilde{\varepsilon}) = 0$, and expanding $\Psi(\varepsilon_1, \varepsilon_2)$ about $\tilde{\varepsilon}$ within the range $\varepsilon - \tilde{\varepsilon} = O(n^{-2/3})$, the bundle strength can be deduced (Daniels, 1989).

The values of C and δ in eqn (10) are obtained (Daniels, 1989; Amaniampong, 1992) from the relation:

$$\Psi'(\tilde{\varepsilon}, \tilde{\varepsilon}) = C[1-(\tilde{\varepsilon}-\varepsilon_0)/\delta], \quad \dot{\Psi}(\tilde{\varepsilon}, \tilde{\varepsilon}) = -C(\tilde{\varepsilon}-\varepsilon_0)/\delta, \tag{11}$$

where $\Psi'(\varepsilon_1, \varepsilon_2) = \partial\Psi/\partial\varepsilon_1$ and $\dot{\Psi}(\varepsilon_1, \varepsilon_2) = \partial\Psi/\partial\varepsilon_2$.

For brevity, the quantities $\Psi(\tilde{\varepsilon}, \tilde{\varepsilon})$, $\Psi'(\tilde{\varepsilon}, \tilde{\varepsilon})$ and $\dot{\Psi}(\tilde{\varepsilon}, \tilde{\varepsilon})$ are represented by Ψ, Ψ' and $\dot{\Psi}$ and $\tau = \varepsilon - \varepsilon_0$. The following cases are then identified (Daniels, 1989; Amaniampong, 1992):

(1) if $\Psi' > 0$ and $\dot{\Psi} < 0$ the system is defined by a Brownian bridge $B(\tau)$;
(2) if $\Psi' > 0$ and $\dot{\Psi} = 0$ the system is defined by a Brownian motion $W(\tau)$; and
(3) if $\Psi' > 0$ and $\dot{\Psi} > 0$ the system is defined by the process analogous to a Brownian bridge $Y(\tau)$.

In each case, $C = \Psi' - \dot{\Psi}$.

By choosing $\eta(\varepsilon) = \mu(\varepsilon) - \mu(\varepsilon^*)$, we get $\eta(\varepsilon^*) = 0$ and $\eta'(\varepsilon^*) = 0$ so the conditions for the curve $-n^{1/2}\eta(\varepsilon)$ which is superimposed on the process are fulfilled. Here ε^* is the value at which $\mu(\varepsilon)$ achieves its maximum value. The maximum load carried by the bundle is asymptotically normally distributed with expected value, $E[L_n^*]$, and variance, $\mathrm{Var}[L_n^*]$, given as

$$\begin{aligned} E[L_n^*] &= n\mu(\tilde{\varepsilon}) + \rho n^{1/3} C^{2/3}[-\mu''(\tilde{\varepsilon})]^{-1/3} \\ \mathrm{Var}[L_n^*] &= n\Psi(\tilde{\varepsilon}, \tilde{\varepsilon}), \end{aligned} \tag{12}$$

where $\tilde{\varepsilon} = \varepsilon^*$ and $\rho = 0.99615\ldots$ is a constant (Daniels, 1989). The mean and the variance of the bundle strength are subsequently given (Amaniampong and Burgoyne, 1992) by

$$\begin{aligned} E[S_n^*] &= \{\mu(\tilde{\varepsilon}) + \rho n^{-2/3} C^{2/3}[-\mu''(\tilde{\varepsilon})]^{-1/3}\}/\mu_a \\ \mathrm{Var}[S_n^*] &= \Psi(\tilde{\varepsilon}, \tilde{\varepsilon})/n\mu_a^2, \end{aligned} \tag{13}$$

where μ'' is the second derivative of the function μ.

To apply eqn (13) to the present bundle the following expressions for Ψ', $\dot{\Psi}$, μ' and μ'' are first obtained (Amaniampong, 1992), using the method adopted by Daniels (1989):

$$\Psi'_{\tilde{\varepsilon}} = \mu_{2a} \int_0^{\min(\varepsilon_1, \theta_{\max})} \left\{ \int \cdots \int \left[\sum_{i=1}^{m} \alpha_i i(\tilde{\varepsilon}-\theta)^{i-1} \right] \times \left[\sum_{i=1}^{m} \alpha_i (\tilde{\varepsilon}-\theta)^i \right] \mathrm{d}B(\underline{\alpha}^t) \right\} [1 - H(\tilde{\varepsilon}-\theta)]\, \mathrm{d}G(\theta) \tag{14}$$

$$\dot{\Psi}_{\tilde{\varepsilon}} = \Psi'_{\tilde{\varepsilon}} - \mu_{2a} \int_0^{\min(\varepsilon_1, \theta_{\max})} \left\{ \int \cdots \int \left[\sum_{i=1}^{m} \alpha_i (\tilde{\varepsilon}-\theta)^i \right]^2 \mathrm{d}B(\underline{\alpha}^t) \right\} [H'(\tilde{\varepsilon}-\theta)]\, \mathrm{d}G(\theta) \tag{15}$$

$$\begin{aligned} \mu'(\varepsilon) = \mu_a &\int_0^{\min(\varepsilon, \theta_{\max})} \left\{ \int \cdots \int \left[\sum_{i=1}^{m} \alpha_i i(\varepsilon-\theta)^{i-1} \right] \mathrm{d}B(\underline{\alpha}^t) \right\} [1 - H(\varepsilon-\theta)]\, \mathrm{d}G(\theta) \\ &+ \mu_a \int_0^{\min(\varepsilon, \theta_{\max})} \left\{ \int \cdots \int \left[\sum_{i=1}^{m} \alpha_i (\varepsilon-\theta)^i \right] \mathrm{d}B(\underline{\alpha}^t) \right\} [-H'(\varepsilon-\theta)]\, \mathrm{d}G(\theta). \end{aligned} \tag{16}$$

If $\int \cdots \int \sum_{i=1}^{m} \alpha_i i(\varepsilon-\theta)^{i-1}\, \mathrm{d}B(\underline{\alpha}^t) = \nabla_1$ and $\int \cdots \int \sum_{i=1}^{m} \alpha_i (\varepsilon-\theta)^i\, \mathrm{d}B(\underline{\alpha}^t) = \nabla_2$, then

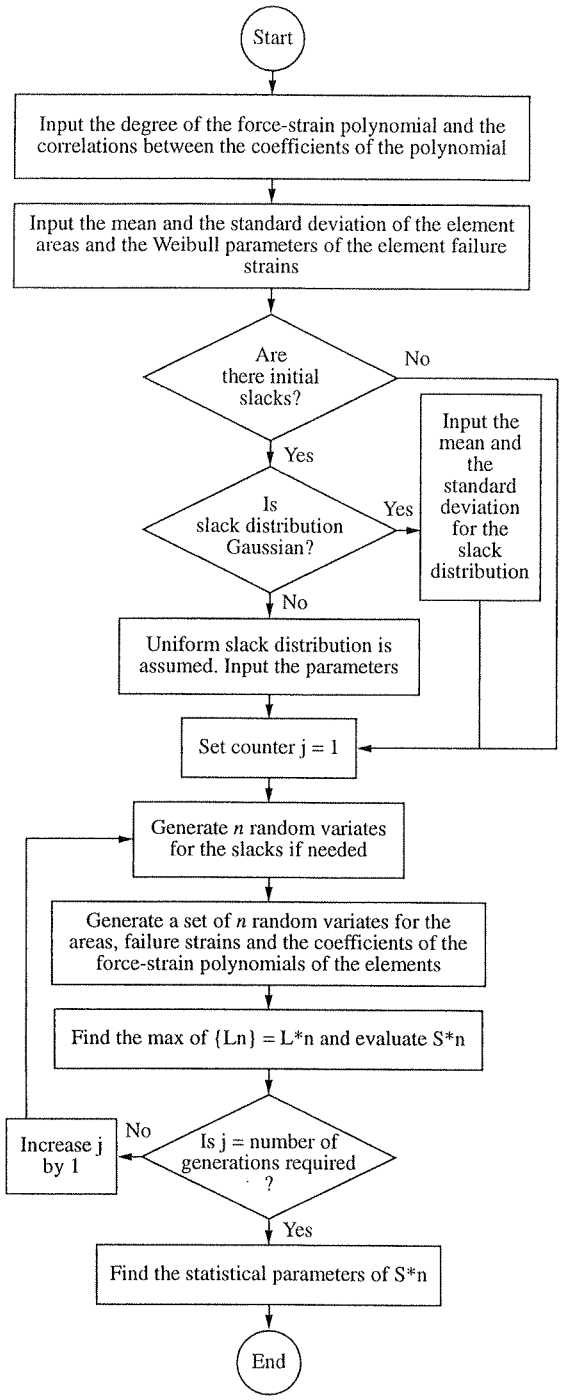

Fig. 2. Flow chart showing the algorithm for the Monte-Carlo simulations.

$$q_m(z) = mq_1(z)[1 - Q_1(z)]^{m-1} \tag{19}$$

with the cumulative distribution function

$$Q_m(z) = 1 - [1 - Q_1(z)]^m. \tag{20}$$

The mean, μ, and the variance, σ^2, of the strength of the long rope can then be calculated from

$$\mu''(\varepsilon) = \mu_a \int_0^{\min(\varepsilon,\theta_{\max})} \left\{ \int \cdots \int \left[\sum_{i=1}^{m} \alpha_i i(i-1)(\varepsilon-\theta)^{i-2} \right] \mathrm{d}B(\underline{\alpha}') \right\}$$

$$\times [1-H(\varepsilon-\theta)]\,\mathrm{d}G(\theta) + \mu_a \int_0^{\min(\varepsilon,\theta_{\max})} 2\nabla_1[-H'(\varepsilon-\theta)]\,\mathrm{d}G(\theta)$$

$$+ \mu_a \int_0^{\min(\varepsilon,\theta_{\max})} \nabla_2[-H''(\varepsilon-\theta)]\,\mathrm{d}G(\theta). \qquad (17)$$

Equations (14)–(17) can be obtained by differentiating eqns (8) and (9) and noting that $\varepsilon_1 \leqslant \varepsilon_2$, $\mu'(\tilde{\varepsilon}) = 0$, $\Psi'_{\tilde{\varepsilon}} = \partial\Psi(\tilde{\varepsilon},\tilde{\varepsilon})/\partial\varepsilon_1$ and $\dot{\Psi}_{\tilde{\varepsilon}} = \partial\Psi(\tilde{\varepsilon},\tilde{\varepsilon})/\partial\varepsilon_2$.

Equation (16) is used to find $\tilde{\varepsilon}$ such that $\mu'(\varepsilon) = 0$. $\mu''(\tilde{\varepsilon})$, $C = \Psi' - \dot{\Psi}$ and $\mu(\tilde{\varepsilon})$ are obtained from eqns (17), (14) and (15), and (8) respectively. These values are then inserted into eqn (13) to obtain the asymptotic bundle strength, which must be evaluated numerically, as described by Amaniampong (1992).

2.3. *Monte-Carlo study of the bundle strength*

As stated previously, an exact evaluation of the bundle strength is impracticable and therefore Monte-Carlo simulations can be used to study the behaviour of small and moderately sized bundles. This is more practical, but there is the drawback of having to specify the probabilistic distributions and the numerical values for the associated parameters of the element characteristics. The statistical distributions used for the present study were obtained from the experimental results discussed by Amaniampong (1992) and Amaniampong and Burgoyne (1992).

For the Monte-Carlo simulation model adopted (Fig. 2), there is the need to specify the correlation between the coefficients of the force–strain polynomials of the elements. The means and the variances of the coefficients are also required. By specifying the numerical values for the required parameters for the chosen statistical distributions representing the failure strains, areas and slack of the bundle elements, the values $\zeta_1, \ldots, \zeta_n$, $a_1, \ldots, a_n$, $\theta_1, \ldots, \theta_n$ and $\underline{\alpha}'_1, \ldots, \underline{\alpha}'_n$ can be generated.

Equations (2) and (3) are applied to evaluate $L_n(\varepsilon)$, the bundle load at strain ε, and the bundle strength, $S_n^* = \sup\{L_n(\varepsilon)/n\mu_a\}$, is obtained, where μ_a is the mean area of the bundle elements. The process is repeated to generate a large number of S_n^* and the data are used with standard statistical inferences about the distribution of the bundle strength.

2.4. *Strength of long ropes*

The asymptotic and the Monte-Carlo methods discussed earlier refer to ropes of a characteristic length. In this section consideration is extended to long ropes.

If an element of a bundle of parallel elements or a yarn of a parallel-lay rope fails, its strain drops to zero and therefore relative movement between the elements ensues. Resistance to the movement is developed because of adhesion, interlocking of the elements or frictional effects.

Over a long rope, the resistance accumulates so that the strain in the failed element develops to the same level as that in the neighbouring elements. There must exist a characteristic length, ℓ^*, within which any element failure causes a loss in strength only over that length; outside this length the element is fully effective.

A long rope is therefore idealized into a number of units, where the length of each unit is that of the characteristic length. Within each unit, any broken element is assumed to have lost its strength only over the unit but becomes fully effective outside that unit.

If the distribution of the strength for each unit is given by the density function, $q_1(z)$, with the cumulative distribution function

$$Q_1(z) = \int_{-\infty}^{z} q_1(z)\,\mathrm{d}z \qquad (18)$$

then, in accordance with the weakest-link concept, the probability density function of the long rope with length $l = m\ell^*$ is given by

$$\mu = \int_{-\infty}^{\infty} z q_m(z)\,\mathrm{d}z$$

$$\sigma^2 = \int_{-\infty}^{\infty} (z-\mu)^2 q_m(z)\,\mathrm{d}z. \tag{21}$$

Equation (21) is not easy to solve (even numerically) as m increases. It is therefore convenient to introduce a new variable $\chi = mQ_1(z)$ so that

$$q_m(z) = \frac{\mathrm{d}\chi}{\mathrm{d}z}\left(1-\frac{\chi}{m}\right)^{m-1}. \tag{22}$$

As m increases

$$q_m(z) = \lim_{m\to\infty} \frac{\mathrm{d}\chi}{\mathrm{d}z}\left(1-\frac{\chi}{m}\right)^{m-1} = \frac{\mathrm{d}\chi}{\mathrm{d}z}\mathrm{e}^{-\chi}. \tag{23}$$

The mean, μ, and the variance, σ^2, of the long rope therefore become

$$\mu = \int_0^m z\,\mathrm{e}^{-\chi}\,\mathrm{d}\chi$$

$$\sigma^2 = \int_0^m z^2\,\mathrm{e}^{-\chi}\,\mathrm{d}\chi - \mu^2, \tag{24}$$

where z is given asymptotically by Epstein (1948) as

$$z = \mu_c - \sigma_c\sqrt{(2\ln m)} + \sigma_c\frac{\ln(\ln m)+\ln(4\pi)}{2\sqrt{(2\ln m)}} + \frac{\sigma_c}{\sqrt{(2\ln m)}}\ln\chi. \tag{25}$$

Here μ_c and σ_c are the mean strength and the standard deviation of the characteristic length, respectively. Equation (24) can then be solved numerically by the Gauss–Laguerre quadrature formula.

3. RESULTS

The results which follow are based on yarn data from tests carried out on Kevlar-49 aramid yarns and high tenacity polyester by Amaniampong (1992) and Amaniampong and Burgoyne (1994). The stress–strain curve of the aramid yarns was best fitted by a third-order polynomial, but that of the polyester yarns was modelled with a fifth-order polynomial without the third and the fourth coefficients (Amaniampong, 1992). The bundles refer to Parafil Type G and A ropes. A yarn is considered as the basic element of the ropes.

Figure 3 shows comparisons between the results of the Monte-Carlo and the asymptotic methods for Type G and A ropes. The failure strains of the yarns obey the conventional two-parameter Weibull distribution (Amaniampong, 1992). The shape and the scale parameters are 18.72 and 1.78% for Type G, and 15.30 and 11.29% for Type A yarns. The strengths predicted by the asymptotic model are higher than those of the Monte-Carlo method for the sizes of Type G rope considered, but the reverse is seen for Type A rope. However, the differences are slight, the maximum being 2 and 1%, respectively.

The differences in the results can be attributed to the fact that the accuracy of the Monte-Carlo simulations depends on the number of times the bundle strengths are generated. This is because the statistical inferences and estimates are made from this number of generations; the greater the number of the bundle strengths generated the better the

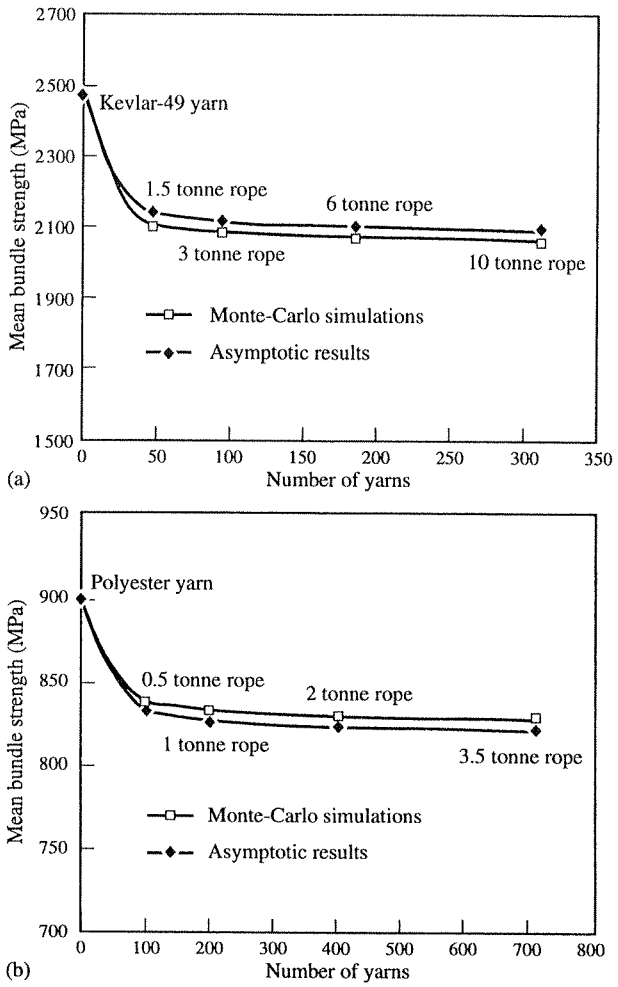

Fig. 3. Comparison of Monte-Carlo simulations with results from bundle theory.

estimates will be. Five hundred and 200 bundle strengths were generated for the estimation of the mean strengths of the Type G and A ropes, respectively. Kolmogorov–Smirnov tests conducted confirm that the bundle strengths are normally distributed for all the sizes of ropes considered. The asymptotic results can be said to be valid for parallel-lay ropes with as few as 50 elements, since the asymptotic bundle strength for 1.5 tonne Type G rope, which is estimated to consist of 47 yarn elements, agrees well with the Monte-Carlo bundle strength.

The mean strengths of 5 tonne Type A [not shown in Fig. 3(b)] and 6 tonne Type G ropes estimated from the model are 821.6 and 2103.0 MPa, respectively. The corresponding values from the tensile tests of the ropes are 820.5 and 2023.2 MPa (Chambers, 1986; Amaniampong, 1992). Although the theoretical (model) results are slightly higher than the empirical ones, the agreement is quite remarkable, giving maximum relative errors of 0.1 and 4%, respectively. The validity of model prediction of bundle strength from the constituent elements is therefore confirmed.

The standard deviations of the tensile strengths of 5 tonne Type A and 6 tonne Type G ropes estimated from the asymptotic model are 9.20 and 33.59 MPa, respectively. The corresponding experimental values are 38.70 and 26.84 MPa. The variability from the model seems not to agree very well with the experimental values, particularly for Type A ropes. Detailed analyses of the variability are presented by Amaniampong (1992).

In Fig. 4 the relationship between the bundle strength and the rope size as well as the results from the classical bundle are presented. The failure stress of the rope decreases with increasing rope size and becomes asymptotic to the failure stress of the classical bundle.

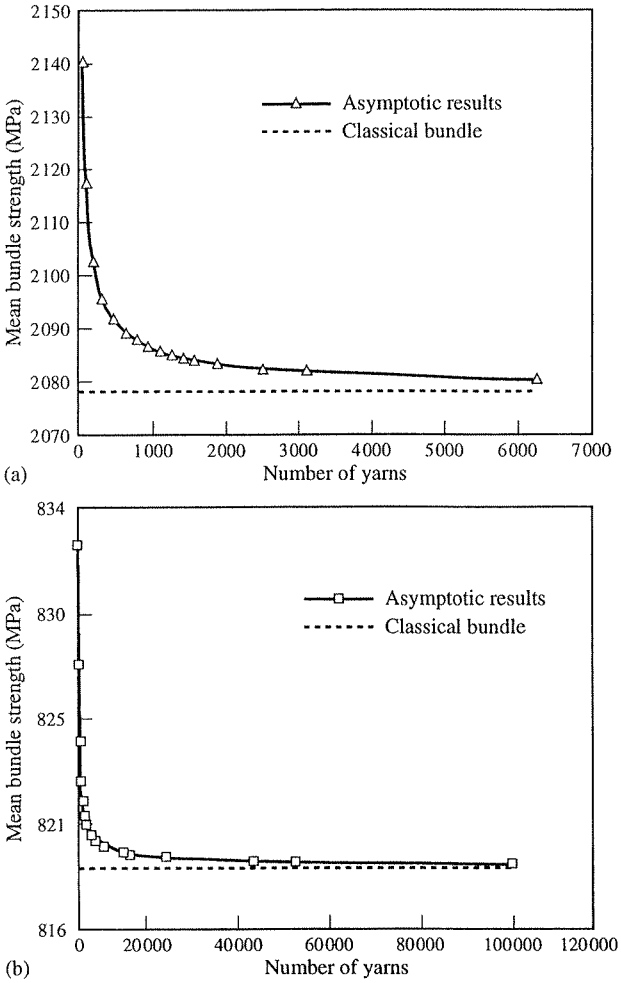

Fig. 4. Size effect of parallel-lay ropes.

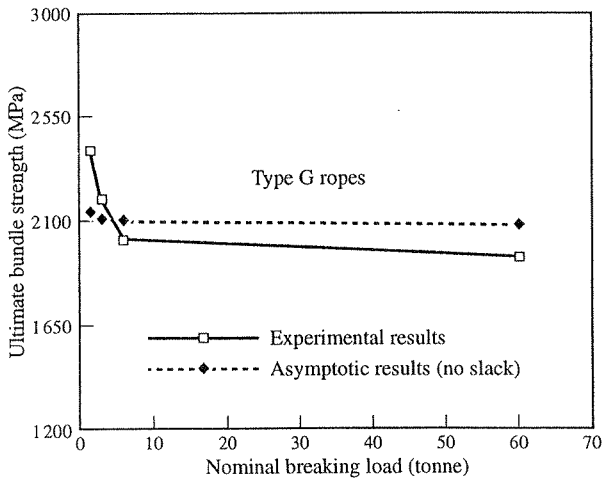

Fig. 5. Comparison of theoretical and experimental results for Type G ropes.

In Fig. 5 there is a comparison between the asymptotic and empirical results from the literature for Type G ropes (Chambers, 1986; Guimarães, 1988b). The maximum relative errors of the results lie in the range 4–11%. Although there are differences, the theory agrees reasonably well with the empirical results. The agreement is even better when the

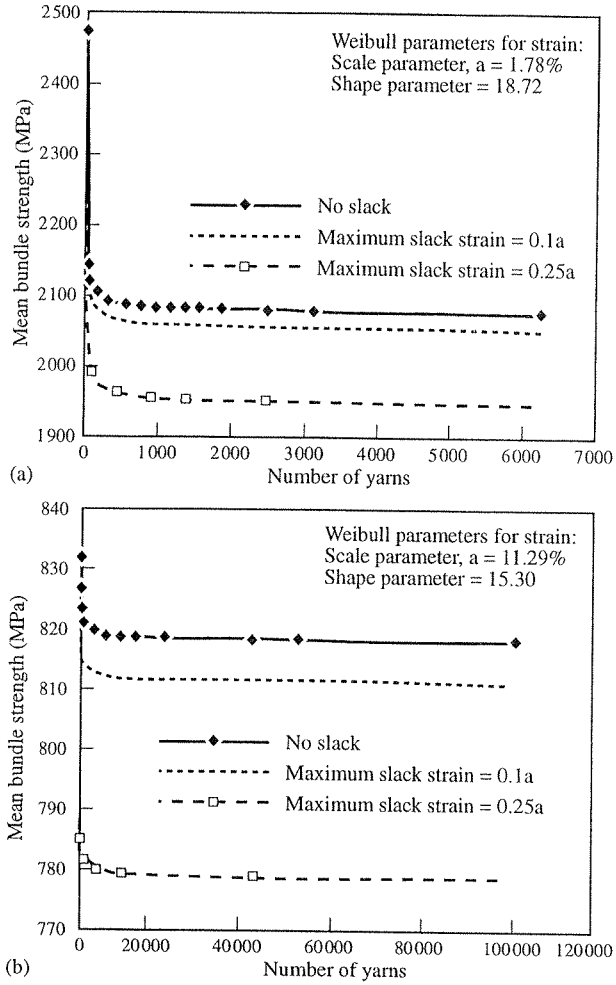

Fig. 6. Effect of slack on parallel-lay ropes (slack is uniformly distributed between zero and the maximum value).

scatter in the rope strength is taken into consideration. The tensile tests of Type G ropes were done after pre-conditioning the ropes, i.e. the ropes were pre-tensioned before the tensile tests were carried out, but the yarns used in the theory were not pre-conditioned. Pre-conditioning is known to affect the behaviour of synthetic materials (Northolt and Van der Hout, 1985) and this could account for the differences. The numbers of yarns per rope for the tested ropes are not given in the literature, so the numbers assumed for the analysis may actually be different, which would also affect the results.

Figure 6 shows the effect of random element slack on the bundle strength. A uniformly distributed random slack was assumed for the elements; the parameters used are shown in Fig. 6. Although a specific slack distribution is desirable, such a distribution is dependent on the manufacturing process, to which access was not permitted. The uniform distribution is chosen mainly because it gives well-defined upper and lower bounds. Other slack distributions can be used, but it is expected that the trend of results will be essentially the same. The variability in the element slack has a profound reducing effect on the strength of the bundle. For instance, introducing a uniform slack distribution with a maximum slack of a quarter of the strain Weibull scale parameter reduces the bundle strength by about 6%. The introduction of a constant slack, however, has no effect on the bundle strength, since a constant slack corresponds only to a displacement on the strain axis.

The effect of the variability in the element cross-sectional area on the strength of parallel-lay ropes is shown in Fig. 7. At low variability (coefficient of variation $<10\%$) in the cross-sectional areas there is an insignificant effect on the bundle strength, but there is

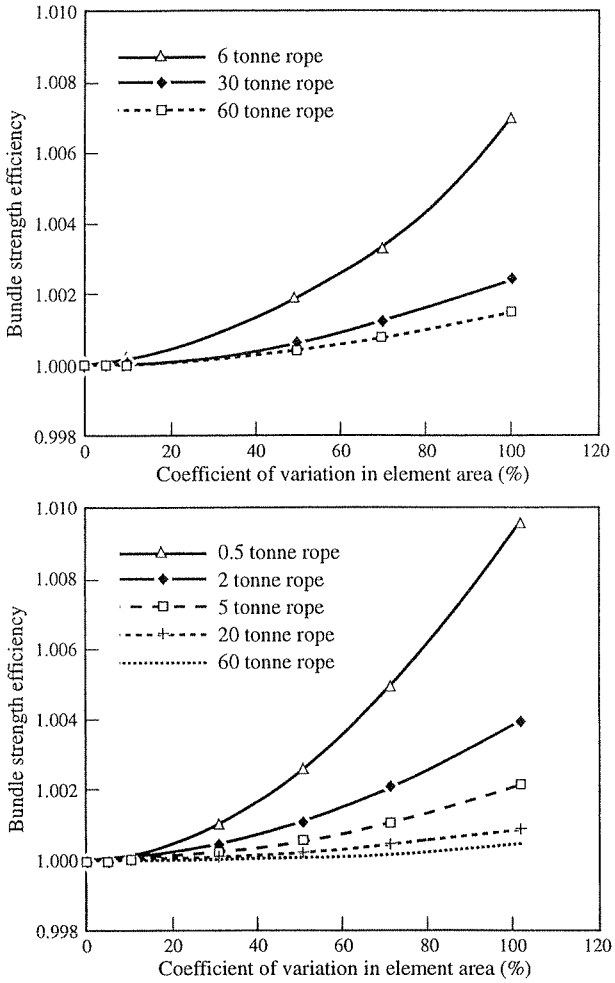

Fig. 7. Effect of the variation in area on the strength of parallel-lay ropes.

a mild increase in bundle strength as the scatter in the cross-sectional areas of the elements increases. The resulting increase in the bundle strength is milder for large ropes. An appreciable effect is observed only for small bundles with very high coefficients of variation in area.

In Fig. 8, the effect of the variability of element stiffness is depicted. Different effects are observed for Type G and A ropes; whereas the strength of Type G ropes increases as the scatter in the element stiffness increases, the reverse is observed for Type A ropes. This is probably related to the degree of the stress–strain polynomial used. The effect is not negligible and therefore any calculation based on the assumption that the elements have constant stiffness may grossly over- or under-estimate the strength of the rope.

The effect of the length on the bundle strength is shown in Fig. 9. Increasing the length of the rope reduces the strength; however, the reduction in strength with increasing length is milder for the large ropes than for the smaller ones. This is because the variability in strength at the characteristic length is higher in smaller ropes than in larger ones.

A parallel-series model is used to predict the strength of long ropes. The longer the rope, the more chance there is of a weak link. Larger bundles, with more elements, more closely approximate the infinite distribution of fibre strength, so variability of strength reduces as the rope gets larger. This in turn means that the distribution of link strengths is lower, so the weak link effect is less pronounced. A further demonstration of the effect is given by Burgoyne and Flory (1990). The characteristic length of Type G rope is estimated as 6.2 m (Burgoyne and Flory, 1990). By using this value, it is predicted that a 6 tonne

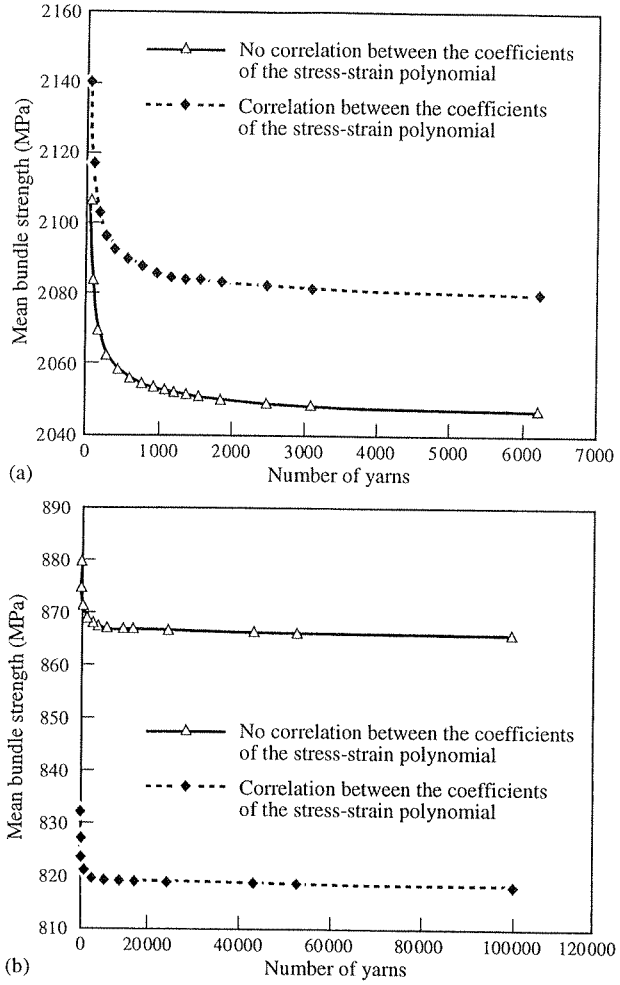

Fig. 8. Effect of the variation in stiffness on the bundle strength.

Type G rope loses about 5% of its characteristic strength (strength at length shorter than 6.2 m) over 3 km, whereas a 60 tonne rope loses only about 2% of its characteristic strength over the same length. It would then follow that large ropes of reasonable length fail at higher stresses than small ropes, which is a reverse of the effect observed on short specimens tested in the laboratory.

4. CONCLUSIONS

A model has been presented for the analysis of the short-term strength of parallel-lay ropes and bundles of parallel elements in general. The model allows analysis of parallel-lay ropes with a non-linear stress–strain relationship and permits study of the variability effects as a result of the scatter in the elements' cross-sectional areas, failure strains, stiffnesses and slack. The following conclusions can be drawn from the work described in this paper:

(1) The present bundle theory predicts reasonably well the mean strengths of parallel-lay ropes. Both the longitudinal and the lateral size effects are predicted by the theory.

(2) The variabilities in element stiffnesses, cross-sectional areas and random slacks affect the bundle strength. The introduction of variable random slack reduces the strength of the rope (bundle). The scatter in the element cross-sectional area increases the bundle strength slightly; however, this increase is only significant at very high variability and

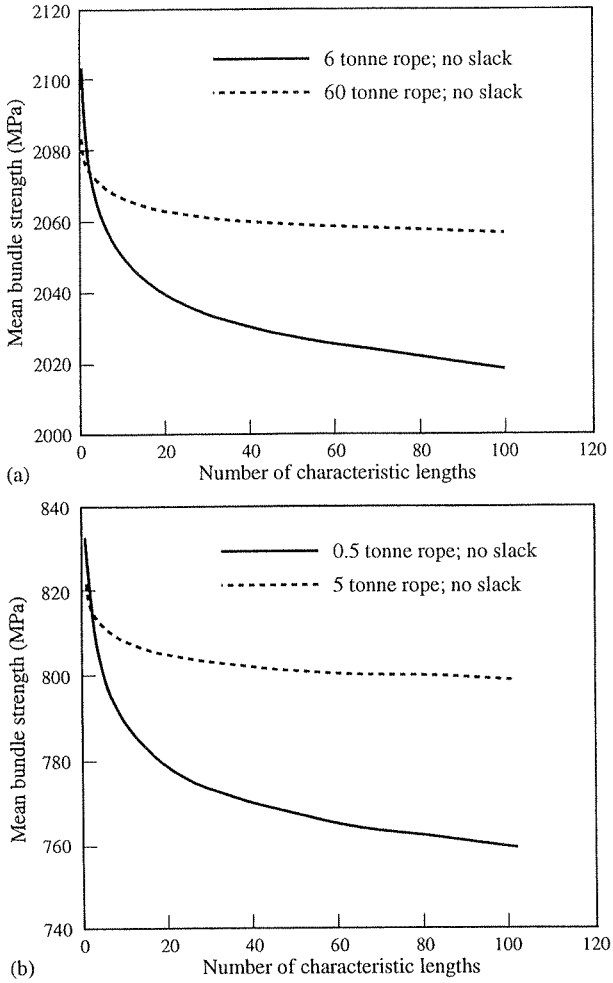

Fig. 9. Effect of length variation on the strength of parallel-lay ropes.

therefore the effect can be considered to be practically insignificant. The effect of the variability in the stiffnesses has different effects on the ropes; whereas Type G rope gains strength, Type A rope loses strength with increasing scatter in element stiffnesses.

(3) Increasing the length of the rope reduces the strength; larger ropes lose strength less rapidly than smaller ones as the length increases. Typically, a 60 tonne Type G rope loses only about 2% of its characteristic strength over 3 km.

Acknowledgements—The tests were carried out in the Cambridge University Structures Research Laboratory, and the Parafil ropes and yarn samples were provided by Linear Composites, whose assistance is gratefully acknowledged. The financial assistance granted by the King's College, Cambridge, is also gratefully acknowledged.

REFERENCES

Amaniampong, G. (1992). Variability and viscoelasticity of parallel-lay ropes. Ph.D. Thesis, University of Cambridge.

Amaniampong, G. and Burgoyne, C. J. (1992). Probabilistic strength analysis of parallel-lay ropes. *Proceedings of the 33rd AIAA, ASME, ASCE, AHS, ASC Structures, Structural Dynamics and Materials Conference*, Vol. 5, pp. 2864–2870. Dallas, Texas.

Amaniampong, G. and Burgoyne, C. J. (1994). Statistical variability in strength and failure strain of aramid and polyester yarns. *J. Mater. Sci.* **29**, 5141–5152.

Baxter, C. (1988). Uses of Parafil ropes for mooring offshore platforms. *Proceedings of the Symposium on Engineering Applications of Parafil Ropes*, pp. 49–62. Imperial College London.

Burgoyne, C. J. (1988). Structural application of Type G Parafil ropes. *Proceedings of the Symposium on Engineering Applications of Parafil Ropes*, pp. 39–47. Imperial College London.

Burgoyne, C. J. and Flory, J. F. (1990). Length effects due to yarn variability in parallel-lay ropes. *Sci. Technol. New Decade, Conf. Proc. MTS* **1**, 49–55.

Chambers, J. J. (1986). Parallel-lay aramid ropes for use as tendons in prestressed concrete. Ph.D. Thesis, University of London.
Coleman, B. D. (1958). On the strength of classical fibres and fibre bundle. *J. Mech. Phys. Solids* **7,** 60–70.
Daniels, H. E. (1945). The statistical theory of strength of bundles of thread I. *Proc. R. Soc.* **A183,** 45–70.
Daniels, H. E. (1989). The maximum of a Gaussian process whose mean path has a maximum with an application to the strength of bundles of fibres. *Adv. Appl. Probab.* **21,** 315–333.
Epstein, B. (1948). Statistical aspects of fracture problems. *J. Appl. Phys.* **19,** 140–147.
Griffith, A. A. (1921). The phenomena of rupture flow in solids. *Phil. Trans. R. Soc. Lond.* **22**(1a), 163–198.
Guimarães, G. B. (1988a). Short-term properties of Parafil. *Proceedings of the Symposium on Engineering Applications of Parafil Ropes*, pp. 13–19. Imperial College London.
Guimarães, G. B. (1988b). Parallel-lay aramid ropes for use in structural engineering. Ph.D. Thesis, University of London.
Harlow, D. G. and Yukich, J. E. (1993). Empirical process methods for classical fiber bundles. *Stochastic Proc. Applic.* **14,** 141–158.
Hult, J. and Travnicek, L. (1983). Carrying capacity of fibre bundles with varying strength and stiffness. *J. Méch. Théor. Appliquée*, **2,** 643–657.
Karlin, S. and Taylor, H. M. (1981). *A Second Course in Stochastic Process*. Academic Press, New York.
Kingston, D. (1988). Development of parallel fibre tensile members. *Proceedings of the Symposium on Engineering Applications of Parafil Ropes*, pp. 7–11. Imperial College London.
Lane, S. H. and Kempton, G. T. (1988). Soil walls—a geotechnical application for synthetic fibres. *Proceedings of the Symposium on Engineering Application of Parafil Ropes*, pp. 85–99. Imperial College London.
Northolt, M. G. and Van der Hout, R. (1985). Elastic extension of an oriented crystalline fibre. *Polymer* **26,** 310–316.
Phoenix, S. L. (1974). Probabilistic strength analysis of fibre bundle structures. *Fibre Sci. Technol.* **7,** 15–31.
Phoenix, S. L. (1975). Probability inter-fiber dependence and the asymptotic strength distribution of classic fiber bundles. *Int. J. Engng Sci.* **13,** 287–304.
Phoenix, S. L. and Taylor, H. M. (1973). The asymptotic strength distribution of general fibre bundle. *Adv. Appl. Probab.* **5,** 200–216.
Pitt, R. E. and Phoenix, S. L. (1981). On modelling the statistical strength of yarns and cables under localized load-sharing amongst fibres. *Text. Res. J.* 408–425.
Wagner, H. D. (1989). Stochastic concepts in the study of size effects in mechanical strength of highly oriented polymeric materials. *J. Polym. Sci.: Part B Polym. Phys.* **27,** 115–149.
Wagner, H. D., Phoenix, S. L. and Schwartz, P. (1984). A study of structural variability in strength of single aramid filaments. *J. Compos. Mater.* **18,** 312–338.